15

Using the Liquid Crystal Spatial Light Modulators for Control of Coherence and Polarization of Optical Beams

Andrey S. Ostrovsky, Carolina Rickenstorff-Parrao
and Miguel Á. Olvera-Santamaría
Universidad Autónoma de Puebla, Facultad de Ciencias Físico Matemáticas
Mexico

1. Introduction

Beginning from the mid-1980's the liquid crystal (LC) spatial light modulators (SLMs) have been used in many optical applications, such as optical data processing, beam shaping, optical communication, adaptive optics, real-time holography, etc. In these applications LC-SLMs are used for both amplitude and phase modulation of optical field. The modulation characteristics of LC- SLMs have been widely studied and reported (Lu & Saleh, 1990). A special attention has been given to the optimization of LC-SLM parameters in order to provide the amplitude-only and phase-only modes of modulation (Yamauchi & Eiju, 1995).

Recently, in connection with the heightened interest in the vector coherence theory of electromagnetic fields (Ostrovsky et al, 2009a), a new possible application of LC-SLMs has been found. It has been shown (Shirai & Wolf, 2004) that LC-SLM of certain configuration can realize the controlled changes of statistical properties of an electromagnetic beam, namely the degree of coherence and the degree of polarization. This fact can be successfully used for generating a secondary partially coherent and partially polarized optical source with the desired characteristics. Somewhat later the technique proposed by Sahirai and Wolf has been improved using the systems of two LC-SLMs coupled in series (Ostrovsky et al., 2009b) or in parallel (Shirai et al., 2005). Unfortunately, the mentioned techniques have not been yet realized in practice because of the lack of commercial LC-SLMs with proper characteristics. Here we propose an alternative technique that uses widely available commercial LC-SLMs and, hence, can be easily realized in practice.

In this chapter, we present a comparative analysis of the techniques for controlling coherence and polarization by LC SLMs. When doing this we consider both the known, properly referenced, techniques and the original ones proposed by the authors. We illustrate the efficiency of the proposed technique with the results of numerical simulation and physical experiments. To facilitate the perception of material, we anticipate the main matter by the backgrounds concerning the fundamentals of vector coherence theory and the elements of theory and design of LC-SLMs. We hope that this chapter will help the specialists and postgraduate students in optics and optoelectronics to be well guided in the subject dispersed in numerous publications.

2. Fundamentals of the unified theory of coherence and polarization

As well known (Wolf, 2007), the second-order statistical properties of a random planar (primary or secondary) electromagnetic source can be completely described by the so-called cross-spectral density matrix

$$\mathbf{W}(\mathbf{x}_1,\mathbf{x}_2)=\begin{pmatrix}\left\langle E_x^*(\mathbf{x}_1)E_x(\mathbf{x}_2)\right\rangle & \left\langle E_x^*(\mathbf{x}_1)E_y(\mathbf{x}_2)\right\rangle\\ \left\langle E_y^*(\mathbf{x}_1)E_x(\mathbf{x}_2)\right\rangle & \left\langle E_y^*(\mathbf{x}_1)E_y(\mathbf{x}_2)\right\rangle\end{pmatrix}, \tag{1}$$

where $E_x(\mathbf{x})$ and $E_y(\mathbf{x})$ are the orthogonal components of the electric field vector $\mathbf{E}(\mathbf{x})$, asterisk denotes the complex conjugate and the angle brackets denote the average over the statistical ensemble (here and further on, for the sake of simplicity, we omit the explicit dependence of the considered quantities on frequency ν). Using this matrix, the following three fundamental statistical characteristics of the source can be defined:
the power spectrum

$$S(\mathbf{x})=\mathrm{Tr}\mathbf{W}(\mathbf{x},\mathbf{x}), \tag{2}$$

the spectral degree of coherence

$$\mu(\mathbf{x}_1,\mathbf{x}_2)=\frac{\mathrm{Tr}\mathbf{W}(\mathbf{x}_1,\mathbf{x}_2)}{[\mathrm{Tr}\mathbf{W}(\mathbf{x}_1,\mathbf{x}_1)\mathrm{Tr}\mathbf{W}(\mathbf{x}_2,\mathbf{x}_2)]^{1/2}}, \tag{3}$$

and the spectral degree of polarization

$$P(\mathbf{x})=\left(1-\frac{4\mathrm{Det}\mathbf{W}(\mathbf{x},\mathbf{x})}{[\mathrm{Tr}\mathbf{W}(\mathbf{x},\mathbf{x})]^2}\right)^{1/2}. \tag{4}$$

In Eqs. (2) - (4) Tr stands for the trace and Det denotes the determinant.
It may be shown that $0\le\left|\mu(\mathbf{x}_1,\mathbf{x}_2)\right|\le 1$ and $0\le P(\mathbf{x})\le 1$. It is said that an electromagnetic source is completely coherent and completely polarized if $\left|\mu(\mathbf{x}_1,\mathbf{x}_2)\right|=1$ and $P(\mathbf{x})=1$, whereas, when $\left|\mu(\mathbf{x}_1,\mathbf{x}_2)\right|=0$ and $P(\mathbf{x})=0$, a source is referred as completely incoherent and completely unpolarized, respectively. In the case of intermediate values of μ and P a source is referred as partially coherent and partially polarized.
As a typical example of such a source, which will be used bellow, we mention the so-called Gaussian Schell-model source (Wolf, 2007) which, in particular case, is given by the diagonal cross-spectral density matrix

$$\mathbf{W}(\mathbf{x}_1,\mathbf{x}_2)=\begin{pmatrix}W_{xx}(\mathbf{x}_1,\mathbf{x}_2) & 0\\ 0 & W_{yy}(\mathbf{x}_1,\mathbf{x}_2)\end{pmatrix} \tag{5}$$

with elements

$$W_{ii}(\mathbf{x}_1,\mathbf{x}_2)=S_{0i}\exp\left(-\frac{\mathbf{x}_1^2+\mathbf{x}_2^2}{4\sigma^2}\right)\exp\left(-\frac{(\mathbf{x}_1-\mathbf{x}_2)^2}{2\sigma_i^2}\right),\quad i=x,y, \tag{6}$$

where S_{0i}, σ_i and σ are positive constants.. It should be noted that the degree of coherence and the degree of polarization of this source take a rather simple form, i.e.

$$\mu(\mathbf{x}_1,\mathbf{x}_2)=\frac{1}{S_{0x}+S_{0y}}\left[S_{0x}\exp\left(-\frac{\xi^2}{2\sigma_x^2}\right)+S_{0y}\exp\left(-\frac{\xi^2}{2\sigma_y^2}\right)\right], \tag{7}$$

$$P(\mathbf{x})=\frac{\left|S_{0x}-S_{0y}\right|}{S_{0x}+S_{0y}}, \tag{8}$$

where $\xi=\left|\mathbf{x}_1-\mathbf{x}_2\right|$.

Now we consider the propagation of the electromagnetic beam characterized by the cross-spectral density matrix $\mathbf{W}(\mathbf{x}_1,\mathbf{x}_2)$ through a thin polarization-dependent screen whose amplitude transmittance is given by the so-called Jones matrix (Yariv & Yeh, 1984)

$$\mathbf{T}(\mathbf{x})=\begin{pmatrix}t_{xx}(\mathbf{x}) & t_{xy}(\mathbf{x})\\ t_{yx}(\mathbf{x}) & t_{yy}(\mathbf{x})\end{pmatrix}, \tag{9}$$

with elements $t_{ij}(\mathbf{x})$ being the random (generally complex) functions of time. It can be readily shown (Shirai & Wolf, 2004) that the cross-spectral density matrix of the beam just behind the screen is given by the expression

$$\mathbf{W}'(\mathbf{x}_1,\mathbf{x}_2)=\left\langle\mathbf{T}^{\dagger}(\mathbf{x}_1)\mathbf{W}(\mathbf{x}_1,\mathbf{x}_2)\mathbf{T}(\mathbf{x}_2)\right\rangle, \tag{10}$$

where the dagger denotes the Hermitian conjugation and the angle brackets again denote the average over the statistical ensemble. Taking into account Eq. (10) with due regard for definitions given by Eqs. (3) and (4), it becomes obvious that, in general, $\mu'(\mathbf{x}_1,\mathbf{x}_2)\neq\mu(\mathbf{x}_1,\mathbf{x}_2)$ and $P'(\mathbf{x})\neq P(\mathbf{x})$. This fact can be used to realize the modulation of coherence and polarization by means of a random polarization-dependent screen. To minimize the light loss, the elements of the matrix $\mathbf{T}(\mathbf{x})$ must be of the form

$$t_{ij}(\mathbf{x})=\exp\left[i\varphi(\mathbf{x})\right], \tag{11}$$

where $\varphi(\mathbf{x})$ is some real random function. To provide the desired statistical characteristics of modulation, the function $\varphi(\mathbf{x})$ has to be generated by computer. The most appropriate candidate for physical realization of such a computer controled random phase screen is the LC-SLM.

3. Elements of the theory and design of LC-SLMs

The LC represents an optically transparent material that has physical properties of both solids and liquids. The molecules of such a material have an ellipsoidal form with a long axis about which there is circular symmetry in any transverse plane. The spatial organization of these molecules defines the type of LC (Goodman, 1996). From the practical point of view, the most interesting type is so-called nematic LC, for which the molecules have a parallel orientation with randomly located centres within entire volume of the material. Further we will consider the LCs exclusively of this type.

Because of its geometrical structure the nematic LC exhibits anisotropic optical behaviour, possessing different refractive indices for light polarized in different directions. From the optical point of view the nematic LC can be considered as an uniaxial crystal with ordinary

refraction index n_o along the short molecular axis and extraordinary refraction index n_e along the long molecular axis, so that it can be characterized by the so-called birefringence parameter

$$\beta = \frac{\pi d}{\lambda}(n_e - n_o), \tag{12}$$

where λ is the wavelength of light and d is the thickness of LC layer.
When LC material is placed in a container with two glass walls it receives the name of LC cell. The glass walls of the LC cell are linearly polished to provide the selected directions in which the LC molecules are aligned at the boundary layers. If the glass walls are polished in different directions, then LC molecules inside the cell gradually rotate to match the boundary conditions at the alignment layers, as illustrated in Fig. 1. Such a LC cell received the name of twisted LC cell. The angle ϕ between the directions of polishing is refered as the twist angle.

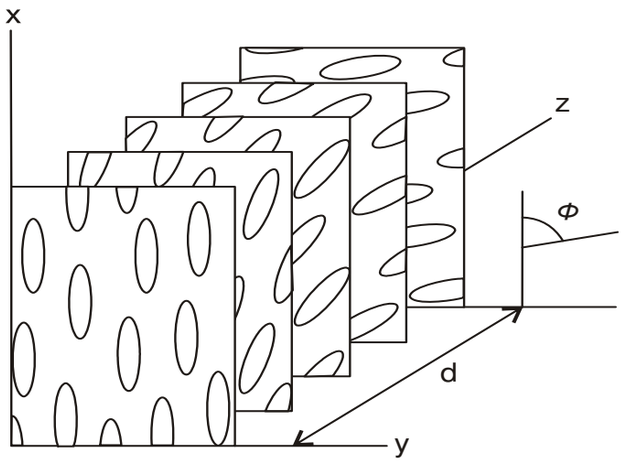

Fig. 1. Twist of LC molecules due to the boundary conditions at the alignment layers.

According to (Yariv & Yeh, 1984), the amplitude transmittance of twisted LC cell with front molecules aligned along *x*-axis is given by the Jones matrix

$$\mathbf{J}_{LC} = \mathbf{R}(-\phi)\exp(-i\beta)\begin{pmatrix} \cos\gamma - i\frac{\beta}{\gamma}\sin\gamma & \frac{\phi}{\gamma}\sin\gamma \\ -\frac{\phi}{\gamma}\sin\gamma & \cos\gamma + i\frac{\beta}{\gamma}\sin\gamma \end{pmatrix}, \tag{13}$$

where

$$\mathbf{R}(\phi) = \begin{pmatrix} \cos(\phi) & \sin(\phi) \\ -\sin(\phi) & \cos(\phi) \end{pmatrix}, \tag{14}$$

is the coordinate rotation matrix and parameter γ is defined as

$$\gamma = \sqrt{\beta^2 + \phi^2}\ . \tag{15}$$

Bellow we consider two important particular cases, namely when $\phi = 0^o$ and $\phi = 90^o$. In the first case we will reffer to the LC cell as 0^o-twist LC cell and in the second case we will refer to it as 90^o-twist LC cell.
For 0^o-twist LC cell Eq. (13) takes the form

$$\mathbf{J}_{\mathrm{LC}} = \begin{pmatrix} \exp(-i2\beta) & 0 \\ 0 & 1 \end{pmatrix}. \tag{16}$$

As can be seen from Eq. (16), the element j_{xx} of matrix $\mathbf{J}_{\mathrm{LC}}$ describes the phase-only modulation, and hence, under certain conditions, the 0^o-twist LC cell can be used to provide the modulation of coherence and polarization discussed in the previous section.
For 90^o-twist LC cell Eq. (13) takes the form

$$\mathbf{J}_{\mathrm{LC}} = \exp(-i\beta)\begin{pmatrix} \dfrac{\pi}{2\gamma}\sin\gamma & -\cos\gamma - i\dfrac{\beta}{\gamma}\sin\gamma \\ \cos\gamma - i\dfrac{\beta}{\gamma}\sin\gamma & \dfrac{\pi}{2\gamma}\sin\gamma \end{pmatrix}, \tag{17}$$

with

$$\gamma = \sqrt{\beta^2 + (\pi/2)^2}\ . \tag{18}$$

As can be seen from Eq. (17), the general element j_{ij} of matrix $\mathbf{J}_{\mathrm{LC}}$ this time describes the joint amplitude and phase modulation, and hence, the 90^o-twist LC cell can not be directly used to realize the modulation of coherence and polarization. Nevertheless, placing the 90^o-twist LC cell between a pair of polarizers whose main axes make angles ψ_1 and ψ_2 with x direction, as is shown in Fig. 2, it is possible to achieve the phase-only modulation (Lu & Saleh, 1990).

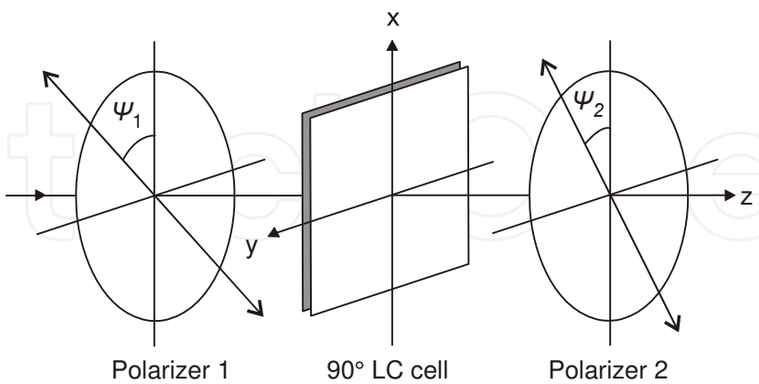

Fig. 2. 90^o-twist LC cell sandwiched between two polarizers.

The Jones matrix for the system shown in Fig. 2 is given by

$$\mathbf{T} = \mathbf{J}_{\mathrm{P}}(\psi_2)\mathbf{J}_{\mathrm{LC}}\mathbf{J}_{\mathrm{P}}(\psi_1)\ , \tag{19}$$

where $\mathbf{J}_{\mathrm{LC}}$ is the matrix given by Eq. (17) and

$$\mathbf{J}_{\mathrm{P}}(\psi)=\begin{pmatrix}\cos^2\psi & \cos\psi\sin\psi\\ \cos\psi\sin\psi & \sin^2\psi\end{pmatrix} \tag{20}$$

is the Jones matrix of polarizer. On substituting from Eqs. (17) and (20) into Eq. (19) with values $\psi_1=0°$ and $\psi_2=90°$, we obtain

$$\mathbf{T}=\exp(-i\beta)\begin{pmatrix}0 & 0\\ \cos\gamma-i\dfrac{\beta}{\gamma}\sin\gamma & 0\end{pmatrix}. \tag{21}$$

The matrix given by Eq. (21) contains the only non-zero element

$$t_{yx}=\exp(-i\beta)\left[\cos\gamma-i\frac{\beta}{\gamma}\sin\gamma\right], \tag{22}$$

which can be expressed in the complex exponential form

$$t_{yx}=\left|t_{yx}\right|\exp\left[-i\arg(t_{yx})\right], \tag{23}$$

with modulus

$$\left|t_{yx}\right|=\left[1-\left(\frac{\pi}{2\gamma}\right)^2\sin^2\gamma\right]^{1/2}, \tag{24}$$

and argument

$$\arg(t_{yx})=\beta+\tan^{-1}\left(\frac{\beta}{\gamma}\tan\gamma\right). \tag{25}$$

The quantities given by Eqs. (24) and (25), as functions of the birefringence parameter β with due regard for Eq. (18), are plotted in Fig. 3.

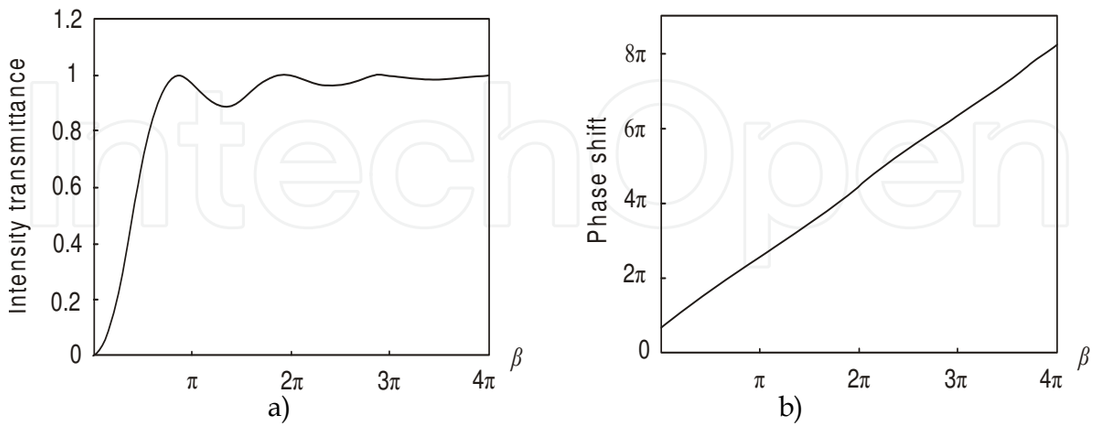

Fig. 3. Complex transmittance given by Eq. (23): a) amplitude transmittance, Eq. (24); b) phase transmittance, Eq. (25).

As can be seen from this figure, starting from some critical value of the birefringence parameter β, approximately equal to $3\pi/2$, the amplitude transmittance $\left|t_{yx}\right|$ approachs to

unity while the phase transmittance rises linearly having a slope of approximately 2β . Thus, when the birefringence parameter satisfies the condition $\beta \geq 3\pi/2$, the matrix given by Eq. (21) can be well approximated as

$$\mathbf{T} = \begin{pmatrix} 0 & 0 \\ \exp(-i2\beta) & 0 \end{pmatrix}, \tag{26}$$

i.e. the 90º-twist LC cell sandwiched between two crossed polarizers can be considered as the phase-only modulator.

Till now we assumed that parameter β characterizing the LC cell has a fixed value. Nevertheless, as well known (Lu & Saleh, 1990) , applying to the LC cell an electric field normal to its surface, the birefringence parameter is no longer constant and changes in accordance with

$$\beta(\delta) = \frac{\pi}{\lambda}[n_{\mathrm{e}}(\delta) - n_{\mathrm{o}}]d \ , \tag{27}$$

where δ is the tilt of the LC molecules with respect to the *z* axis caused by the electric field. Besides, the relationship between extraordinary refraction index and the molecular tilt can be approximated as

$$n_{\mathrm{e}}(\delta) \approx (n_{\mathrm{e}} - n_{\mathrm{o}})\cos^2\delta + n_{\mathrm{o}} \ . \tag{28}$$

It has been shown (Lu & Saleh, 1990) that the dependence between tilt angle and applied voltage has the form

$$\theta(V_{\mathrm{rms}}) = \begin{cases} 0 & , \quad V_{\mathrm{rms}} \leq V_{\mathrm{c}} \\ \dfrac{\pi}{2} - 2\arctan\left\{\exp\left[-\left(\dfrac{V_{\mathrm{rms}} - V_{\mathrm{c}}}{V_0}\right)\right]\right\} & , \quad V_{\mathrm{rms}} > V_{\mathrm{c}} \end{cases}, \tag{29}$$

where V_{c} is the threshold voltage, V_0 is the saturation voltage, and V_{rms} is the effective voltage. Combining Eqs. (27) – (29), it is possible to show that the birefringence parameter β finds to be approximately proportional to the inverse value of the applied voltage.

Finally, we are ready to define a LC-SLM as an electro-optical device composed by a large number of LC cells (pixels) whose birefringence indices are controlled by the electrical signals generated by computer and applied individually to each cell by means of an array of electrodes. The amplitude transmittance of 0º-twist LC-SLM or 90º-twist LC-SLM can be described by Eqs. (16) and (26), respectively, replacing parameter β by spatial function $\beta(\mathbf{x})$.

4. Techniques for control of coherence and polarization by means of LC-SLMs

4.1 Single 0º-twist LC-SLM

We begin with the technique based on the use of a 0º-twist LC-SLM (Shirai & Wolf, 2004). It is assumed that the incident light represents a linear polarized laser beam characterized by the cross-spectral density matrix

$$\mathbf{W}(\mathbf{x}_1,\mathbf{x}_2)=E_0^2\exp\left(-\frac{\mathbf{x}_1^2+\mathbf{x}_2^2}{4\varepsilon^2}\right)\begin{pmatrix}\cos^2\theta & \cos\theta\sin\theta\\ \cos\theta\sin\theta & \sin^2\theta\end{pmatrix}, \tag{30}$$

where E_0 is the value of power spectrum at the beam centre, ε is the effective (rms) size of the source, and θ is the angle that the direction of polarization makes with the x axis. It can be readily verified that for such a beam $\mu(\mathbf{x}_1,\mathbf{x}_2)=1$ and $P(\mathbf{x})=1$, i.e. the beam described by Eq. (30) is completely coherent and completely (linearly) polarized.

If the extraordinary axis of the LC is aligned along the y direction the transmittance of 0°-twist LC-SLM, in accordance with the previous section, is given by matrix

$$\mathbf{T}_{\mathrm{LC1}}(\mathbf{x})=\begin{pmatrix}1 & 0\\ 0 & \exp[-i2\beta_1(\mathbf{x})]\end{pmatrix} \tag{31}$$

(here the subscript "1" is used for the sake of simplicity of posterior consideration). It is assumed that the birefringence $\beta_1(\mathbf{x})$ has the form

$$\beta_1(\mathbf{x})=\frac{1}{2}\left[\varphi_0+\varphi(\mathbf{x})\right], \tag{32}$$

where φ_0 is a constant and $\varphi(\mathbf{x})$ is a computer generated zero mean random variable which is characterized by the Gaussian probability density

$$p\left[\varphi(\mathbf{x})\right]=\frac{1}{\sqrt{2\pi}\sigma_\varphi}\exp\left(-\frac{\varphi^2(\mathbf{x})}{2\sigma_\varphi^2}\right), \tag{33}$$

with variance $\left\langle\varphi^2(\mathbf{x})\right\rangle=\sigma_\varphi^2$ and cross correlation defined at two different points as

$$\left\langle\varphi(\mathbf{x}_1)\varphi(\mathbf{x}_2)\right\rangle=\sigma_\varphi^2\exp\left(-\frac{\xi^2}{2\alpha_\varphi^2}\right), \tag{34}$$

where $\xi=\left|\mathbf{x}_1-\mathbf{x}_2\right|$ and α_φ is a positive constant characterizing correlation width of $\varphi(\mathbf{x})$.

On substituting from Eqs. (30) - (32) into Eq. (10), one obtains

$$\mathbf{W}'(\mathbf{x}_1,\mathbf{x}_2)=E_0^2\exp\left(-\frac{\mathbf{x}_1^2+\mathbf{x}_1^2}{4\varepsilon^2}\right)$$
$$\times\begin{pmatrix}\cos^2\theta & \exp(-i\varphi_0)\left\langle\exp[-i\varphi(\mathbf{x}_2)]\right\rangle\cos\theta\sin\theta\\ \exp(i\varphi_0)\left\langle\exp[i\varphi(\mathbf{x}_1)]\right\rangle\cos\theta\sin\theta & \left\langle\exp\{i[\varphi(\mathbf{x}_1)-\varphi(\mathbf{x}_2)]\}\right\rangle\sin^2\theta\end{pmatrix}. \tag{35}$$

On making use of Eqs. (33) and (34), it can be shown that (Ostrovsky et al, 2009b, 2010)

$$\left\langle\exp[\pm i\varphi(\mathbf{x})]\right\rangle=\exp\left(-\frac{\sigma_\varphi^2}{2}\right), \tag{36}$$

$$\left\langle\exp\{+i\left[\varphi(\mathbf{x}_1)\pm\varphi(\mathbf{x}_2)\right]\}\right\rangle=\left\langle\exp\{-i\left[\varphi(\mathbf{x}_1)\pm\varphi(\mathbf{x}_2)\right]\}\right\rangle=\exp\left\{-\sigma_\varphi^2\left[1\pm\exp\left(-\frac{\xi^2}{2\alpha_\varphi^2}\right)\right]\right\}. \tag{37}$$

Then, Eq. (35) can be rewritten as

$$\mathbf{W}'(\mathbf{x}_1,\mathbf{x}_2) = E_0^2 \exp\left(-\frac{\mathbf{x}_1^2+\mathbf{x}_1^2}{4\varepsilon^2}\right)$$

$$\times \begin{pmatrix} \cos^2\theta & \exp(-i\varphi_0)\exp\left(-\frac{\sigma_\varphi^2}{2}\right)\cos\theta\sin\theta \\ \exp(i\varphi_0)\exp\left(-\frac{\sigma_\varphi^2}{2}\right)\cos\theta\sin\theta & \exp\left\{-\sigma_\varphi^2\left[1-\exp\left(-\frac{\xi^2}{2\alpha_\varphi^2}\right)\right]\right\}\sin^2\theta \end{pmatrix}. \tag{38}$$

To simplify the consequent analysis, we assume that σ_φ is large enough to accept the following approximations (Shirai & Wolf, 2004):

$$\exp\left(-\frac{\sigma_\varphi^2}{2}\right) \approx 0\,, \tag{39}$$

$$\exp\left\{-\sigma_\varphi^2\left[1-\exp\left(-\frac{\xi^2}{2\alpha_\varphi^2}\right)\right]\right\} \approx \exp\left(-\frac{\xi^2}{2\eta_\varphi^2}\right), \tag{40}$$

where $\eta_\varphi = \alpha_\varphi/\sigma_\varphi$. In this case Eq. (38) can be rewritten approximately as

$$\mathbf{W}'(\mathbf{x}_1,\mathbf{x}_2) = E_0^2 \exp\left(-\frac{\mathbf{x}_1^2+\mathbf{x}_1^2}{4\varepsilon^2}\right)\begin{pmatrix} \cos^2\theta & 0 \\ 0 & \exp\left(-\frac{\xi^2}{2\eta_\varphi^2}\right)\sin^2\theta \end{pmatrix}. \tag{41}$$

According to definitions given by Eqs. (3) and (4), we find

$$\mu'(\xi) = 1-\left[1-\exp\left(-\frac{\xi^2}{2\eta_\varphi^2}\right)\right]\sin^2\theta\,, \tag{42}$$

$$P'(\mathbf{x}) = \left|\cos 2\theta\right|. \tag{43}$$

Equations (42) and (43) show that the modulated beam is, in general, partially coherent and partially polarized. The degree of polarization changes in the range from 1 to 0 with a proper choice of polarization angle θ of the incident beam. The degree of coherence, for a fixed value of θ can be varied by a proper choice of parameters α_φ and σ_φ of the control signal $\varphi(\mathbf{x})$, as it is shown in Fig. 4.

We would like to point out the following two shortcomings of the described technique. Firstly, as can be seen from Eqs. (42) and (43) this technique does not provide the independent modulation of the degree of coherence and the degree of polarization since both of them depend at the same time on the polarization angle θ. Secondly, as can be seen from Fig. 4, this technique does not allow to obtain the values of the degree of coherence in a whole desired range from 1 to 0.

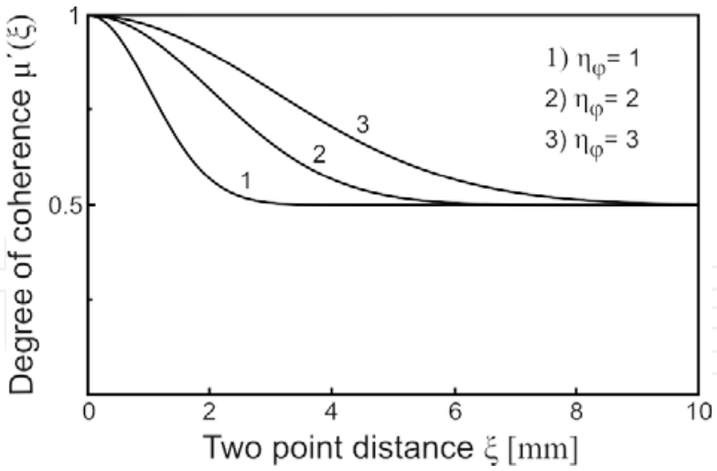

Fig. 4. Degree of coherence given by Eq. (42) for $\theta = \pi/4$ and different values of η_φ.

4.2 Two 0º-twist LC-SLMs coupled in series

To avoid the shortcomings mentioned above, the authors (Ostrovsky et al, 2009) proposed to use instead of a single 0°-twist LC-SLM the system of two 0°-twist LC-SLMs coupled in series as shown in Fig. 5.

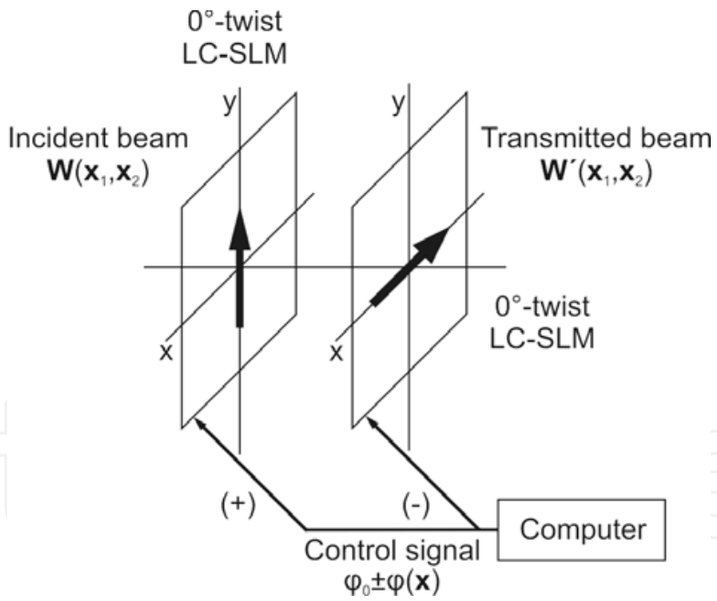

Fig. 5. System of two crossed 0°-twist LC-SLMs coupled in series. The bold-faced arrows denote the extraordinary axis of liquid LC.

The transmittance of the first SLM is just the same as in previous technique, while the transmittance of the second one, whose extraordinary axis is aligned in the x direction, is given by matrix

$$\mathbf{T}_{\mathrm{LC}\,2}(\mathbf{x}) = \begin{pmatrix} \exp[-i2\beta_2(\mathbf{x})] & 0 \\ 0 & 1 \end{pmatrix}, \tag{44}$$

where birefringence $\beta_2(\mathbf{x})$ has the form

$$\beta_2(\mathbf{x}) = \frac{1}{2}\left[\varphi_0 - \varphi(\mathbf{x})\right], \tag{45}$$

with φ_0 and $\varphi(\mathbf{x})$ of the same meaning as stated in the context of Eq. (32). The transmittance of the system composed by two crossed 0º-twist LC-SLMs is given by matrix

$$\mathbf{T}(\mathbf{x}) = \mathbf{T}_{\mathrm{LC2}}(\mathbf{x})\mathbf{T}_{\mathrm{LC1}}(\mathbf{x}) = \exp(-i\varphi_0)\begin{pmatrix} \exp[i\varphi(\mathbf{x})] & 0 \\ 0 & \exp[-i\varphi(\mathbf{x})] \end{pmatrix}. \tag{46}$$

On substituting from Eqs. (30) and (46) into Eq. (10) with due regard for relation (37), one obtains

$$\mathbf{W}'(\mathbf{x}_1,\mathbf{x}_2) = E_0^2 \exp\left(-\frac{\mathbf{x}_1^2+\mathbf{x}_1^2}{4\varepsilon^2}\right)$$

$$\times\begin{pmatrix} \exp\left\{-\sigma_\varphi^2\left[1-\exp\left(-\frac{\xi^2}{2\alpha_\varphi^2}\right)\right]\right\}\cos^2\theta & \exp\left\{-\sigma_\varphi^2\left[1+\exp\left(-\frac{\xi^2}{2\alpha_\varphi^2}\right)\right]\right\}\cos\theta\sin\theta \\ \exp\left\{-\sigma_\varphi^2\left[1+\exp\left(-\frac{\xi^2}{2\alpha_\varphi^2}\right)\right]\right\}\cos\theta\sin\theta & \exp\left\{-\sigma_\varphi^2\left[1-\exp\left(-\frac{\xi^2}{2\alpha_\varphi^2}\right)\right]\right\}\sin^2\theta \end{pmatrix} \tag{47}$$

and then, using approximations (39) and (40),

$$\mathbf{W}'(\mathbf{x}_1,\mathbf{x}_2) = E_0^2 \exp\left(-\frac{\mathbf{x}_1^2+\mathbf{x}_1^2}{4\varepsilon^2}\right)\exp\left(-\frac{\xi^2}{2\eta_\varphi^2}\right)\begin{pmatrix} \cos^2\theta & 0 \\ 0 & \sin^2\theta \end{pmatrix}. \tag{48}$$

According to definitions given by Eqs. (3) and (4), we find

$$\mu'(\xi) = \exp\left(-\frac{\xi^2}{2\eta_\varphi^2}\right), \tag{49}$$

$$P'(\mathbf{x}) = \left|\cos 2\theta\right|. \tag{50}$$

As can be seen from Eqs. (49) and (50), the output degree of coherence in this case does not depend on direction of the input polarization and changes in the whole desired range from 1 to 0.

4.3 Two 0º-twist LC-SLMs coupled in parallel

The result resembling the one given above can be also obtained using the system of two 0º-twist LC-SLMs coupled in parallel. Such a system has been described in (Shirai et al, 2005). Here we propose a somewhat modified version of this technique.

The technique is based on the use of two 0º-twist LC-SLMs with orthogonal orientations of their extraordinary axes placed in the opposite arms of a Mach-Zehnder interferometer as it is shown in Fig. 7. The polarizing beam splitter at the interferometer input separates the orthogonal beam components $E_x(\mathbf{x})$ and $E_y(\mathbf{x})$ so that each of them can be independently

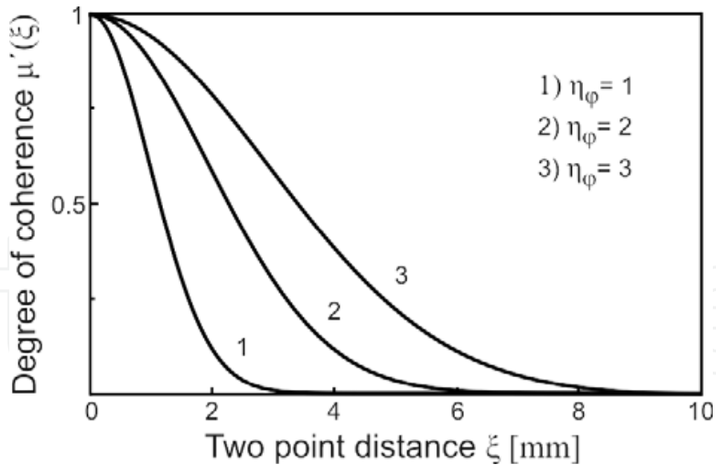

Fig. 6. Degree of coherence given by Eq. (49) for $\theta = \pi/4$ and different values of η_φ.

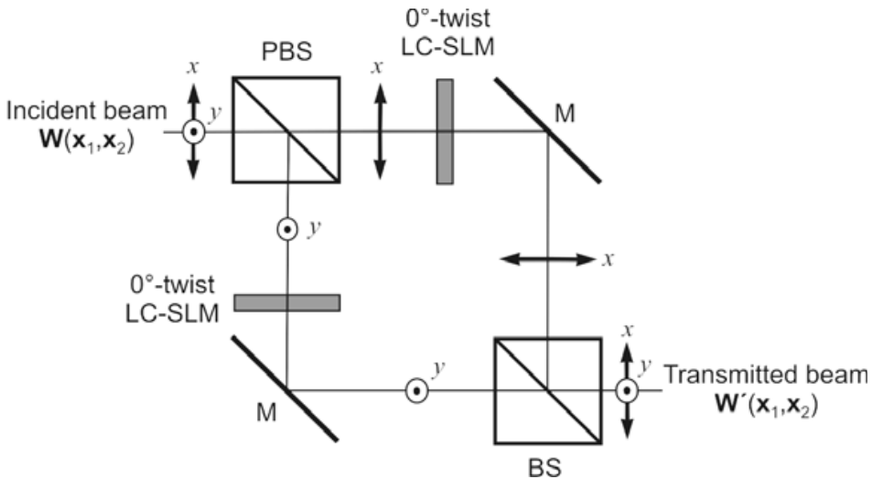

Fig. 7. System of two crossed 0°-twist LC-SLMs coupled in parallel: PBS, polarizing beam splitter; M mirror; BS beam splitter. The bold-faced arrows and circled dots denote polarization directions.

modified by different LC-SLMs. The modified beam components are superimposed in the conventional beam splitter at the interferometer output. Disregarding the negligible changes of coherence and polarization properties of the electromagnetic field induced by the free space propagation within the interferometer, one can represent the considering system as a thin polarization-dependent screen with the transmittance given by matrix

$$\mathbf{T}(\mathbf{x}) = \begin{pmatrix} \exp[-i2\beta_1(\mathbf{x})] & 0 \\ 0 & \exp[-i2\beta_2(\mathbf{x})] \end{pmatrix}. \tag{51}$$

As before, we assume that parameter β of each 0°-twist LC-SLM has the form

$$\beta_{1(2)}(\mathbf{x}) = \frac{1}{2}\left[\varphi_0 + \varphi_{1(2)}(\mathbf{x})\right], \tag{52}$$

with φ_0 and $\varphi_{1(2)}(\mathbf{x})$ of the same meaning as stated in the context of Eq. (32). It is assumed also that the variables $\varphi_1(\mathbf{x})$ and $\varphi_2(\mathbf{x})$ are generated by two different computers so that they can be considered as statistically independent with the separable joint probability density

$$p[\varphi_1(\mathbf{x})\varphi_2(\mathbf{x})] = p[\varphi_1(\mathbf{x})]p[\varphi_2(\mathbf{x})]. \tag{53}$$

Following Subsection 4.1 and using in addition relation (Ostrovsky et al, 2010)

$$\left\langle \exp\{i[\varphi_{1(2)}(\mathbf{x}_2) \pm \varphi_{2(1)}(\mathbf{x}_1)]\}\right\rangle = \exp\left(-\sigma_\varphi^2\right), \tag{54}$$

it may be readily shown that the cross-spectral density matrix $\mathbf{W}'(\mathbf{x}_1,\mathbf{x}_2)$, the degree of coherence $\mu'(\mathbf{x}_1,\mathbf{x}_2)$ and the degree of polarization $P'(\mathbf{x})$, in this case, are just the same as ones given by Eqs. (48) – (50).

4.4 Two 90º-twist LC-SLMs coupled in parallel

The considered above techniques for modulation of coherence and polarization are based on the use of 0º-twist LC-SLMs. The consistence of these techniques is well grounded in theory but no relevant experimental results have been yet reported. This situation can be explained by the lack at present of commercial 0º-twist LC-SLMs with the required characteristics. Here we propose an alternative technique which uses widely available commercial 90º-twist LC-SLMs and, hence, can be easily realized in practice. The proposed technique is sketched schematically in Fig. 8.

In spite of its outward resemblance with the technique described in the previous subsection, this technique has two essential distinctions. Firstly, instead of 0º-twist LC-SLMs here the orthogonally aligned 90º-twist LC-SLMs are used in the opposite arms of the Mach-Zehnder interferometer. Secondly, the conventional beam splitter at the output of interferometer is replaced by the polarizing one. As a result, taking into account that two polarizing beam splitters coupled in series act as crossed polarizers, each arm of interferometer can be considered as the system shown in Fig. 2 with $\psi_1 = 0º$ and $\psi_2 = 90º$. In accordance with Section 3 such a system realizes the phase-only modulation of the correspondent orthogonal component of the incident beam.

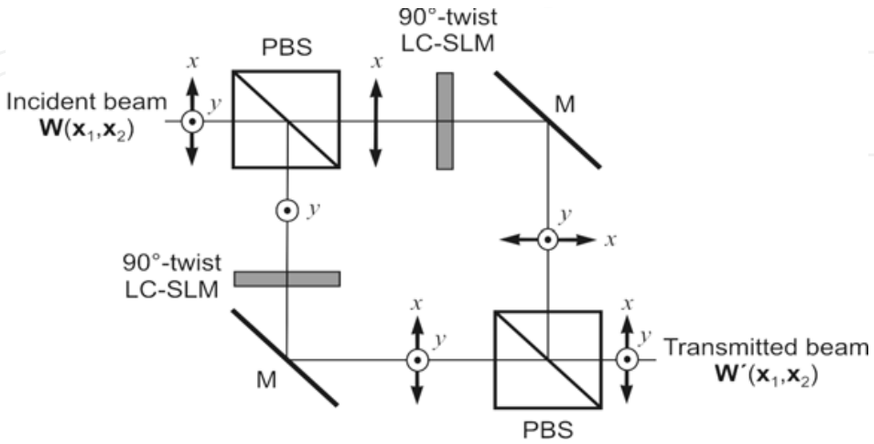

Fig. 8. System of two crossed 90º-twist LC-SLMs coupled in parallel: PBS, polarizing beam splitter; M, mirror. The bold-faced arrows and circled dots denote polarization directions.

Again disregarding the negligible changes of coherence and polarization properties of the electric field induced by the free space propagation within the interferometer, the system shown in Fig. 8 can be considered as a thin polarization-dependent screen with transmittance given by matrix

$$\mathbf{T}(\mathbf{x}) = \begin{pmatrix} 0 & \exp[-i2\beta_2(\mathbf{x})] \\ \exp[-i2\beta_1(\mathbf{x})] & 0 \end{pmatrix}, \tag{55}$$

where $\beta_{1(2)}(\mathbf{x})$ has the same meaning as in Eq. (51). It can be readily shown that for this technique the cross-spectral density matrix has a slightly different form, namely

$$\mathbf{W}'(\mathbf{x}_1,\mathbf{x}_2) = E_0^2 \exp\left(-\frac{\mathbf{x}_1^2+\mathbf{x}_1^2}{4\varepsilon^2}\right)\exp\left(-\frac{\xi^2}{2\eta_\varphi^2}\right)\begin{pmatrix} \sin^2\theta & 0 \\ 0 & \cos^2\theta \end{pmatrix}, \tag{56}$$

but the degree of coherence $\mu'(\mathbf{x}_1,\mathbf{x}_2)$ and the degree of polarization $P'(\mathbf{x})$ are given again by Eqs. (49) and (50).

Concluding, it is appropriate to mention here that the proposed technique, as well the one presented before, provides generating the beam of a Gaussian Schell-model type given by Eq. (6) with parameters $S_{0x} = E_0^2 \sin^2\theta$, $S_{0y} = E_0^2 \cos^2\theta$ and $\sigma_x = \sigma_y = \eta_\varphi$.

5. Measurements of coherence and polarization

In practice the efficiency of the techniques described in previous section can be verified by measuring the degree of coherence and the degree of polarization of modulated electromagnetic beam. The main idea of such a measuring is well known (Wolf, 2007) and consists in the implementation of four two-pinhole Young's experiments with different states of polarization of the radiation emerged from each pinhole. Nevertheless, the practical realization of such an idea proves to be difficult in consequence of physical impossibility to insert the needed optical elements just behind the pinholes. Here we present the technique for measuring the degree of coherence and the degree of polarization proposed by the authors (Ostrovsky et al, 2010), which permits to avoid this difficultness.

The technique consists in applying the Mach-Zehnder interferometer shown in Fig. 9. This allows the physical insertion of the appropriate optical elements for simultaneous and independent transforming the orthogonal beam components. The polarizers P_1 and P_2 serve to cut off only one of the orthogonal field components, while the removable rotators R_1 and R_2 serve to produce the rotation of one of the transmitted field component through 90° (for such a purpose a suitably oriented half-wave plate can be used). The operation description of the technique is given bellow.

The determination of the elements W'_{ij} of the matrix $\mathbf{W}'(\mathbf{x}_1,\mathbf{x}_2)$ is realized by means of the following four experiments. In the first experiment the polarizers P_1 and P_2 are aligned to transmit only x components of the incident field without any subsequent rotation of the plane of polarization. In the second experiment P_1 and P_2 are aligned to transmit only y components of the incident field again without any subsequent rotation of the plane of polarization. In the third and the fourth experiments the polarizers P_1 and P_2 cut off the different orthogonal components of the incident field and the corresponding polarization rotator R_1 or R_2 serves to allow the interference of these components.

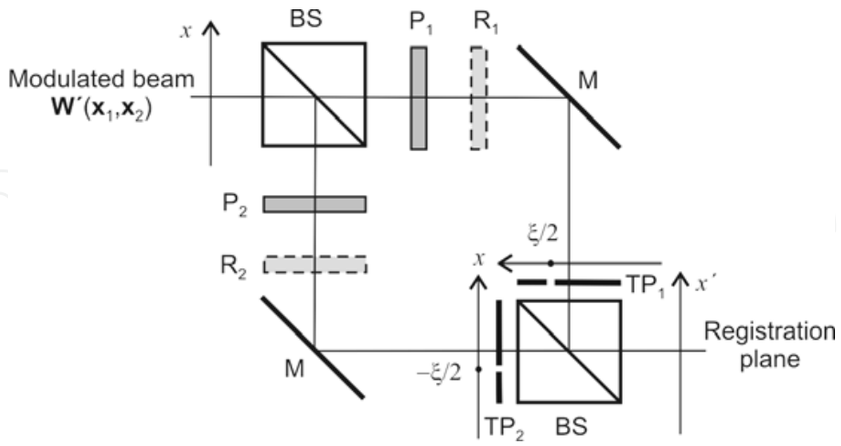

Fig. 9. System for measuring the statistical properties of modulated beam: BS, beam splitter; M, mirror; TP, translating pinhole; P_1, P_2, polarizers; R_1, R_2; polarization rotators.

The spectral density or power spectrum of the field observed at the output of the interference system in each experiment can be described by the spectral interference law, which under certain conditions can be written as (Wolf, 2007)

$$S_{ij}(x') = S_i'\left(\frac{\xi}{2}\right) + S_j'\left(\frac{\xi}{2}\right) + 2\left|W_{ij}'\left(\frac{\xi}{2},-\frac{\xi}{2}\right)\right|\cos\left[\frac{k\xi}{z_0}x' + \alpha_{ij}\left(\frac{\xi}{2},-\frac{\xi}{2}\right)\right] \quad (i,j=x,y), \tag{57}$$

where S_i' and S_j' are the power spectra of the field components in the pinhole position $\xi/2$, k is the wave number, z_0 is the geometrical path between the pinhole plane and the observation plane, and $\alpha_{ij} = \arg W_{ij}'$. From the physical point of view, Eq. (57) describes an image with periodic structure, known as the interference fringe pattern. The measure of the contrast of the interference fringes is the so-called visibility coefficient defined as

$$V_{ij}(\xi) = \frac{S_{ij}'^{\max}(x') - S_{ij}'^{\min}(x')}{S_{ij}'^{\max}(x') + S_{ij}'^{\min}(x')}. \tag{58}$$

On substituting from Eq. (57) with $\cos(.) = \pm 1$ into Eq. (58), we readily find that

$$\left|W_{ij}'(\xi)\right| = \frac{1}{2}\left[S_i'\left(\frac{\xi}{2}\right) + S_j'\left(\frac{\xi}{2}\right)\right]V_{ij}(\xi). \tag{59}$$

The spectra S_i' and S_j' can be easily measured when one of the pinholes is covered by an opaque screen. The phase α_{ij} can be measured by determining the location of maxima in the interference pattern. Hence, measuring in each experiment the visibility V_{ij}, power spectra $S_{i(j)}'$, and phase α_{ij}, one can determine all the elements W_{ij}' of the matrix $\mathbf{W}'(\mathbf{x}_1,\mathbf{x}_2)$. The degree of coherence and the degree of polarization of the modulated beam can be then calculated using definitions given by Eqs. (3) and (4).

6. Experiments and results

To verfy the proposed technique in practice, we conducted some physical experiments. The experimental setup used in experiments is sketched in Fig. 10. The principal part of the experimental setup was composed of two Mach-Zehnder interferometers coupled by the common beam splitter. The first interferometer realized the modulation of the incident beam as it has been described in Subsection 4.4, while the second one served for measuring the degree of coherence and the degree of polarization of the modulated beam as it has been described in Section 5.

As the primary source we used a highly coherent linearly polarized beam generated by He-Ne laser (Spectra-Physics model 117A, λ=633 nm, output power 4.5 mW) which can be well described by the model given by Eq. (30). The laser was mounted in a rotary stage that allowed changing the polarization angle θ without any loss of light energy. As the 90°-twist nematic LC-SLMs we used the computer controlled HoloEye LC2002 electro-optical modulators which have resolution of 800 × 600 pixels (32 μm square in size) and can display the control signal with 8 bit accuracy (256 gray levels). The control of LC-SLMs was realized independently by two computers using a specially designed program for generating the random signals which obey the desired Gaussian statistics. To realize the measurements of the degree of coherence we used two pinholes with diameter of 200 μm mounted on motorized linear translation stages.

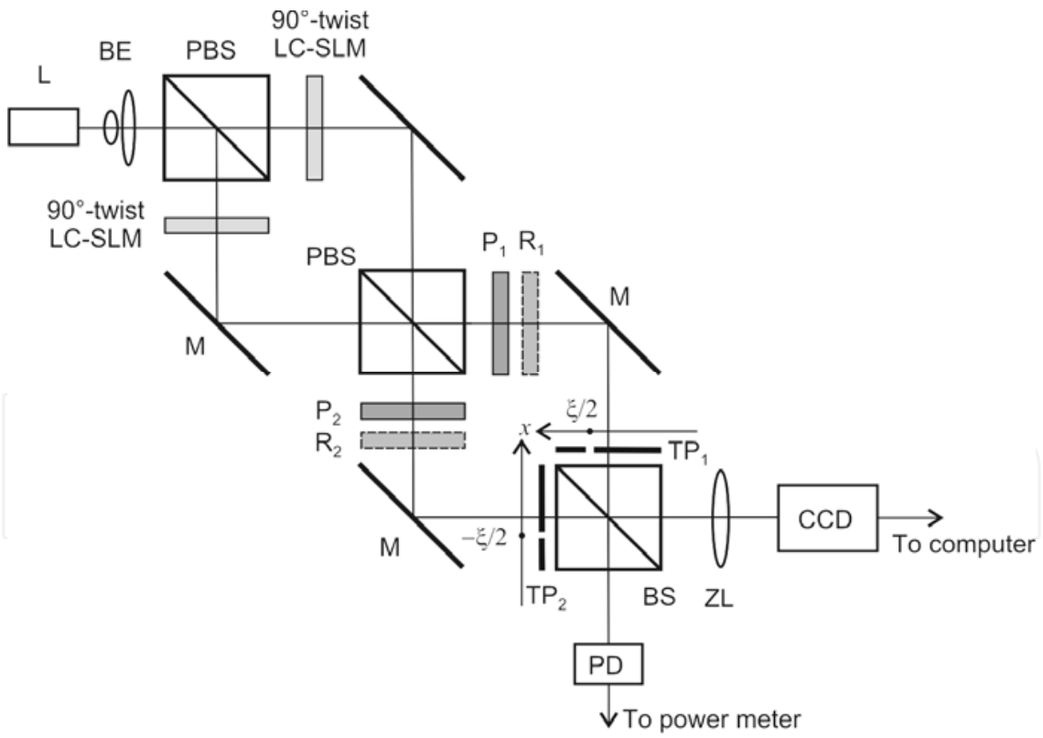

Fig. 10. Experimental setup: L, laser; BE, beam expander; ZL, zoom-lens; PD, photodiode; the other abbreviations are just the same as in Figs. 8 and 9.

We realized two sets of experiments. In the first set we measured the degree of polarization for different values of the polarization angle of incident beam and for the fixed value (≈ 1)

of parameter η_φ of the control signal. The results of these experiments are shown in Fig. 11. In the second set we chosed $\theta = \pi/4$ and measured the degree of coherence varying the parameters α_φ and σ_φ of the control signal to ensure the chosen values of parameter η_φ. The results of these experiments are shown in Fig. 12. As a whole, the results obtained in both sets of experiments are in a good accordance with theoretical predictions.

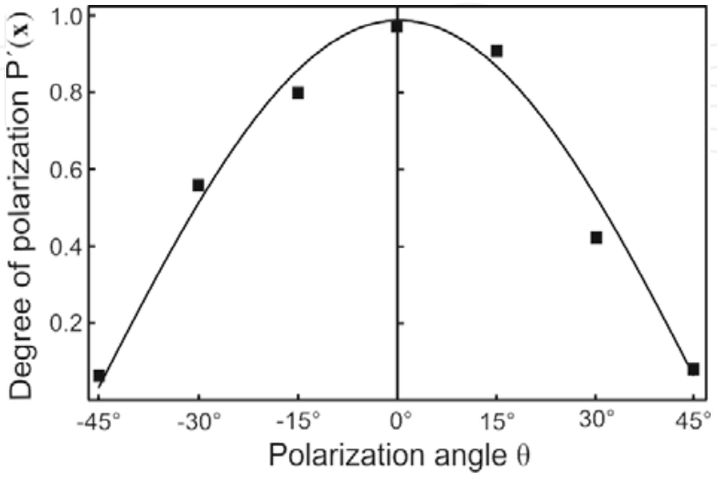

Fig. 11. Results of measuring the degree of polarization for $\eta_\varphi \approx 1$.

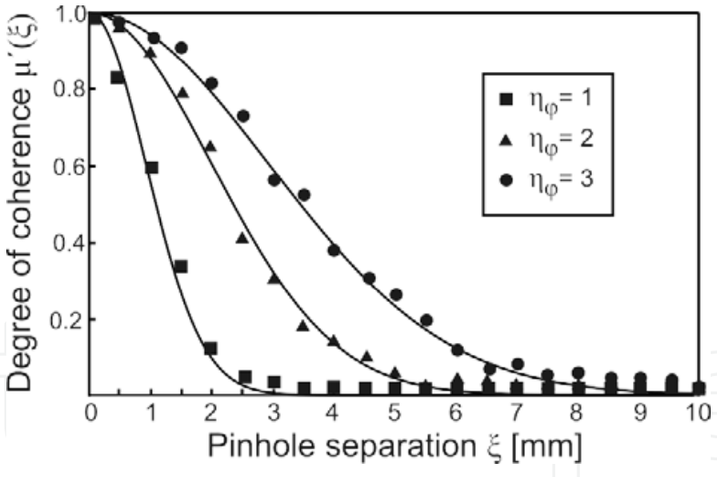

Fig. 12. Results of measuring the degree of coherence for $\theta = \pi/4$ and different values of parameter η_φ.

7. Conclusion

In this chapter the problem of modulating the coherence and polarization of optical beams has been considered. It has been shown that the LC-SLM represents an ideal tool for practical realizing such a modulation. We have analized the known techniques of optical modulation based on the use of 0^o-twist LC-SLM and have proposed a new technique based on the use of two 90^o-twist LC-SLMs. Because of the wide commercial availability of 90^o-

twist LC-SLMs the proposed technique proves to be the most attractive one. The justifiability of this technique has been corroborated by the results of physical experiments.

8. Acknowledgment

The authors gratefully acknowledge the financial support from the Benemérita Universidad Autónoma de Puebla under project VIEP: OSA-EXT-11-G.

9. References

Goodman, J. W. (1996). *Introduction to Fourier Optics* (2nd Edition), McGraw-Hill, ISBN 0-07-024254-2, USA.

Lu, K. & Saleh B. E. A. (1990). Theory and design of the liquid crystal TV as an optical spatial phase modulator. *Optical Engineering,* Vol.29, No.3, (March 1990), pp. (240-246). ISSN 0091-3286.

Ostrovsky A. S. (2006). *Coherent Mode Representations in Optics,* SPIE Press, ISBN 0-8194-6350-7, Bellingham WA, USA.

Ostrovsky A. S. ; Martínez-Vara P. ; Olvera-Santamaría M. Á. & Martínez-Niconoff G. (2009a). Vector coherence theory : An overview of basic concepts and definitions, In: *Recent Research Developments in Optics,* S. G. Pandalai, (113-132), Research Singpost, ISBN 978-81-308-0370-8, Kerala, India

Ostrovsky A. S.; Martínez-Niconoff G.; Arrizón V.; Martínez-Vara P.; Olvera-Santamaría M. Á. & Rickenstorff C. (2009b). Modulation of coherence and polarization using liquid crystal spatial light modulators. *Optics Express,* Vol.17, No.7, (March 2009), pp. (5257-5264). ISSN 1094-4087.

Ostrovsky A. S.; Rodríguez-Zurita G.; Meneses-Fabián C.; Olvera-Santamaría M. Á. & Rickenstorff C. (2010). Experimental generating the partially coherent and partially polarized electromagnetic source. *Optics Express,* Vol.18, No.12, (June 2010), pp.(12864-12871). ISSN 1094-4087.

Shirai T. & Wolf E. (2004). Coherence and polarization of electromagnetic beams modulated by random phase screens and their changes on propagation in free space. *Journal of the Optical Society of America A,* Vol.21, No.10, (October 2004), pp. (1907-1916). ISSN 1084-7529.

Shirai T.; Korotkova O. & Wolf E. (2005). A method of generating electromagnetic Gaussian Schell-model beams. *Journal of Optics A: Pure and Applied Optics,* Vol.7, No.5, (March 2005), pp. (232-237). ISSN 1464-4258.

Wolf E. (2007). *Introduction to the Theory of Coherence and Polarization of Light,* Cambridge University Press, ISBN 9780521822114, Cambridge, UK.

Yamauchi M. & Eiju T. (1995). Optimization of twisted nematic liquid crystal panels for spatial light phase modulation. *Optical Communications,* Vol.115, No.1, (March 1995), pp. (19-25). ISSN 0030-4018.

Yariv, A. & Pochi, Y. (1984). *Optical Waves in Crystals,* Wiley, ISBN 0-471-09142-1, USA.

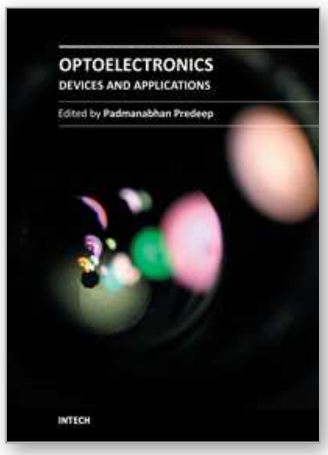

Optoelectronics - Devices and Applications

Edited by Prof. P. Predeep

ISBN 978-953-307-576-1
Hard cover, 630 pages
Publisher InTech
Published online 03, October, 2011
Published in print edition October, 2011

Optoelectronics - Devices and Applications is the second part of an edited anthology on the multifaced areas of optoelectronics by a selected group of authors including promising novices to experts in the field. Photonics and optoelectronics are making an impact multiple times as the semiconductor revolution made on the quality of our life. In telecommunication, entertainment devices, computational techniques, clean energy harvesting, medical instrumentation, materials and device characterization and scores of other areas of R&D the science of optics and electronics get coupled by fine technology advances to make incredibly large strides. The technology of light has advanced to a stage where disciplines sans boundaries are finding it indispensable. New design concepts are fast emerging and being tested and applications developed in an unimaginable pace and speed. The wide spectrum of topics related to optoelectronics and photonics presented here is sure to make this collection of essays extremely useful to students and other stake holders in the field such as researchers and device designers.

InTech Europe
University Campus STeP Ri
Slavka Krautzeka 83/A
51000 Rijeka, Croatia
Phone: +385 (51) 770 447
Fax: +385 (51) 686 166
www.intechopen.com

InTech China
Unit 405, Office Block, Hotel Equatorial Shanghai
No.65, Yan An Road (West), Shanghai, 200040, China
中国上海市延安西路65号上海国际贵都大饭店办公楼405单元
Phone: +86-21-62489820
Fax: +86-21-62489821

IntechOpen